Linear and Nonlinear Inverse Scattering Applied to Experimental Data

René Marklein, ***Jinghong Miao***

University of Kassel, Department of Electrical Engineering / Computer Science, Electromagnetic Theory,
Wilhelmshöher Allee 71, D-34121 Kassel, Germany.
e-mail: marklein@uni-kassel.de, miaojing@uni-kassel.de

Abstract

In this paper, we present our recent work on the imaging techniques for solving the 2–D inverse scattering problems in the frequency and time domain, which is the continuation of our work described in [1]. Two linear algorithms, Synthetic Aperture Focusing Technique (SAFT) and MUltiple SIgnal Classification (MUSIC) algorithm, as well as two nonlinear algorithms, Contrast Source Inversion (CSI) and Multiplicative Regularization Contrast Source Inversion (MR-CSI), are applied to reconstruct the experimental electromagnetic data sets from Institute Fresnel [2], France, and experimental elastic data sets from the Fraunhofer Institute for Non-Destructive Testing (IZFP), Germany.

1. Overview of the Applied Inversion Algorithms

In 2–D, the acoustic case, the electromagnetic transversal magnetic (TM) case, and the elastodynamic horizontally polarized shear (SH) case can be treated as scalar cases. Beside that, the transversal electric (TE) case of electromagnetic waves and the pressure and vertically polarized shear (P–SV) case of elastic waves must be treated as vector cases. Throughout this paper we focus on both cases, the scalar and vector case. Details can be found in [3]. Before we introduce the inverse scattering algorithms, we represent the data and object equations for the 2-D scalar, the TE, and P-SV case. We consider a domain $\mathbb{D}$ with homogeneous background and inhomogeneous scatterer. The data are measured on the surface $\mathbb{M}$ which encloses the domain $\mathbb{D}$. The data and object equations for the 2-D scalar case are

$$\phi^{\mathrm{sc}}(\underline{\mathbf{r}},\omega) = k^2 \iint_{\underline{\mathbf{r}}'\in\mathbb{D}} \chi(\underline{\mathbf{r}}',\omega)\phi(\underline{\mathbf{r}}',\omega)G(\underline{\mathbf{r}}-\underline{\mathbf{r}}',\omega)\,\mathrm{d}^2\underline{\mathbf{r}}' \quad \underline{\mathbf{r}} \in \mathbb{M} \tag{1}$$

$$\phi(\underline{\mathbf{r}},\omega) = \phi^{\mathrm{in}}(\underline{\mathbf{r}},\omega) + k^2 \iint_{\underline{\mathbf{r}}'\in\mathbb{D}} \chi(\underline{\mathbf{r}}',\omega)\phi(\underline{\mathbf{r}}',\omega)G(\underline{\mathbf{r}}-\underline{\mathbf{r}}',\omega)\,\mathrm{d}^2\underline{\mathbf{r}}' \quad \underline{\mathbf{r}} \in \mathbb{D} \tag{2}$$

where G is the 2–D free-space *Green's* function, k is the wavenumber and χ is the contrast function characterized by a difference in material properties with respect to the background. The data and object equations for the TE case are given as

$$\underline{\mathbf{E}}^{\mathrm{sc}}(\underline{\mathbf{r}},\omega) = \left[k_{\mathrm{em}}^2 + \nabla\nabla\right] \cdot \iint_{\underline{\mathbf{r}}'\in\mathbb{D}} \chi(\underline{\mathbf{r}}',\omega)\underline{\mathbf{E}}(\underline{\mathbf{r}}',\omega)G_{\mathrm{em}}(\underline{\mathbf{r}}-\underline{\mathbf{r}}',\omega)\,\mathrm{d}^2\underline{\mathbf{r}}' \quad \underline{\mathbf{r}} \in \mathbb{M} \tag{3}$$

$$\underline{\mathbf{E}}(\underline{\mathbf{r}},\omega) = \underline{\mathbf{E}}^{\mathrm{in}}(\underline{\mathbf{r}},\omega) + \left[k_{\mathrm{em}}^2 + \nabla\nabla\right] \cdot \iint_{\underline{\mathbf{r}}'\in\mathbb{D}} \chi(\underline{\mathbf{r}}',\omega)\underline{\mathbf{E}}(\underline{\mathbf{r}}',\omega)G_{\mathrm{em}}(\underline{\mathbf{r}}-\underline{\mathbf{r}}',\omega)\,\mathrm{d}^2\underline{\mathbf{r}}' \quad \underline{\mathbf{r}} \in \mathbb{D} \tag{4}$$

where k_{em} is the wavenumber of the electromagnetic waves and G_{em} is the 2–D free-space *Green's* function with k replaced by k_{em}. The data and object equations of the P–SV case are given by

$$\begin{aligned}\underline{\mathbf{u}}^{\mathrm{sc}}(\underline{\mathbf{r}},\omega) = &\left[k_{\mathrm{S}}^2 + \nabla\nabla\right] \cdot \iint_{\underline{\mathbf{r}}'\in\mathbb{D}} \chi(\underline{\mathbf{r}}',\omega)\underline{\mathbf{u}}(\underline{\mathbf{r}}',\omega)G_{\mathrm{S}}(\underline{\mathbf{r}}-\underline{\mathbf{r}}',\omega)\,\mathrm{d}^2\underline{\mathbf{r}}' \\ &- \nabla\nabla \cdot \iint_{\underline{\mathbf{r}}'\in\mathbb{D}} \chi(\underline{\mathbf{r}}',\omega)\underline{\mathbf{u}}(\underline{\mathbf{r}}',\omega)G_{\mathrm{P}}(\underline{\mathbf{r}}-\underline{\mathbf{r}}',\omega)\,\mathrm{d}^2\underline{\mathbf{r}}' \quad \underline{\mathbf{r}} \in \mathbb{M}\end{aligned} \tag{5}$$

$$\underline{\mathbf{u}}(\underline{\mathbf{r}},\omega) = \underline{\mathbf{u}}^{\mathrm{in}}(\underline{\mathbf{r}},\omega) + \left[k_{\mathrm{S}}^2 + \nabla\nabla\right] \cdot \iint_{\underline{\mathbf{r}}'\in\mathbb{D}} \chi(\underline{\mathbf{r}}',\omega)\underline{\mathbf{u}}(\underline{\mathbf{r}}',\omega)G_{\mathrm{S}}(\underline{\mathbf{r}}-\underline{\mathbf{r}}',\omega)\,\mathrm{d}^2\underline{\mathbf{r}}'$$

$$- \nabla\nabla \cdot \iint_{\underline{\mathbf{r}}' \in \mathbb{D}} \chi(\underline{\mathbf{r}}', \omega) \underline{\mathbf{u}}(\underline{\mathbf{r}}', \omega) G_{\mathrm{P}}(\underline{\mathbf{r}} - \underline{\mathbf{r}}', \omega) \, \mathrm{d}^2\underline{\mathbf{r}}' \quad \underline{\mathbf{r}} \in \mathbb{D} \tag{6}$$

where G_{S} and G_{P} are the 2–D free-space *Green's* functions for shear and pressure waves, k_{S} is the wavenumber of the shear waves. For the convenience of solving the inverse scattering problems of elastic waves, we can separate the pressure and shear scattered fields in equation (5) by using the properties of pressure and shear waves. We apply the following linear and nonlinear inversion schemes:

- The Synthetic Aperture Focusing Technique (SAFT), which is a linear phenomenological imaging technique in time domain [3, 4].
- The MUltiple SIgnal Classification (MUSIC) algorithm, which is generally used in sub-space signal processing. Here we apply MUSIC to solve the inverse scattering problem. The principle of MUSIC is described in [5, 6, 7].
- The Contrast Source Inversion (CSI) algorithm, proposed in [8], is an iterative algorithm. Object and data equations for different cases are used here [9, 10, 11].
- The Multiplicative Regularized Contrast Source Inversion (MR-CSI) algorithm is the CSI algorithm with multiplicative regularizer. proposed in [12, 13].

2. Inversion Results

Electromagnetic Data: We consider an inhomogeneous target consisting of two smaller circular dielectric cylinders with a contrast $\chi_\epsilon = 2 \pm 0.3$ and a larger circular dielectric cylinder with a contrast $\chi_\epsilon = 0.45 \pm 0.15$; one smaller cylinder is embedded inside the larger cylinder, and another touches the larger cylinder as shown in Fig. 1(a). The inversion results of MUSIC, CSI and MR-CSI at a single frequency of 6 GHz are given in Fig. 1(b)–(f). The inversion results of CSI and MR-CSI using multiple-frequency are given in Fig. 1(g)–(j). We observe from Fig. 1(j) that an excellent reconstruction for location, shape as well as constitutive parameters of the target has been obtained.

Elastic Data: The target consists of six holes filled with water bored in an aluminium background as shown in Fig. 2(a). These six holes measure 2 mm each in diameter. Since the elastic data only contain the normal component with regard to the measurement surfaces, we have another option to treat this problem as a scalar inversion problem. The SAFT reconstruction in Fig. 2(b) shows the result for the complete time-domain data. After a Fourier transform with regard to time, we obtain frequency-domain data as an input for CSI and MR-CSI. The inversion results of CSI and MR-CSI at a single frequency of $f = 2.1$ MHz are given in Fig. 2(c)–(f) and for multiple frequencies are given in Fig. 2(g)–(j). We observe that in Fig. 2(h) the location and shape as well as in Fig. 2(j) the contrast value are reconstructed better.

3. References

1. R. Marklein, K. Balasubramanian, K. J. Langenberg, J. Miao, S. M. Sinaga, "Applied linear and nonlinear scalar inverse scattering", *Proceedings of the XXVIIth General Assembly of URSI*, Maastricht, The Netherlands, 2002.
2. J. M. Geffrin, P. Sabouroux and C. Eyraud, "Free space experimental scattering database continuation: experimental set-up and measurement precision", *Inverse Problems*, Vol. 21, pp. S117-S130, 2005.
3. K. J. Langenberg, M. Brandfass, R. Hannemann, Ch. Hofmann, T. Kaczorowski, J. Kostka, R. Marklein, K. Mayer and A. Pitsch, "Inverse scattering with acoustic, electromagnetic, and elastic waves as applied in Nondestructive Evaluation", *Scalar and Vector Wavefield Inverse Problems*, pp. 59-118, Ed. Armand Wirgin, Springer Publication, Wien, 1999.
4. R. Marklein, K. Mayer, R. Hannemann, T. Krylow, K. Balasubramanian, K. J. Langenberg and V. Schmitz, "Linear and nolinear inversion algorithms applied in nondestructive evaluation", *Inverse Problems*, Vol. 18, pp. 1733-1759, 2002.

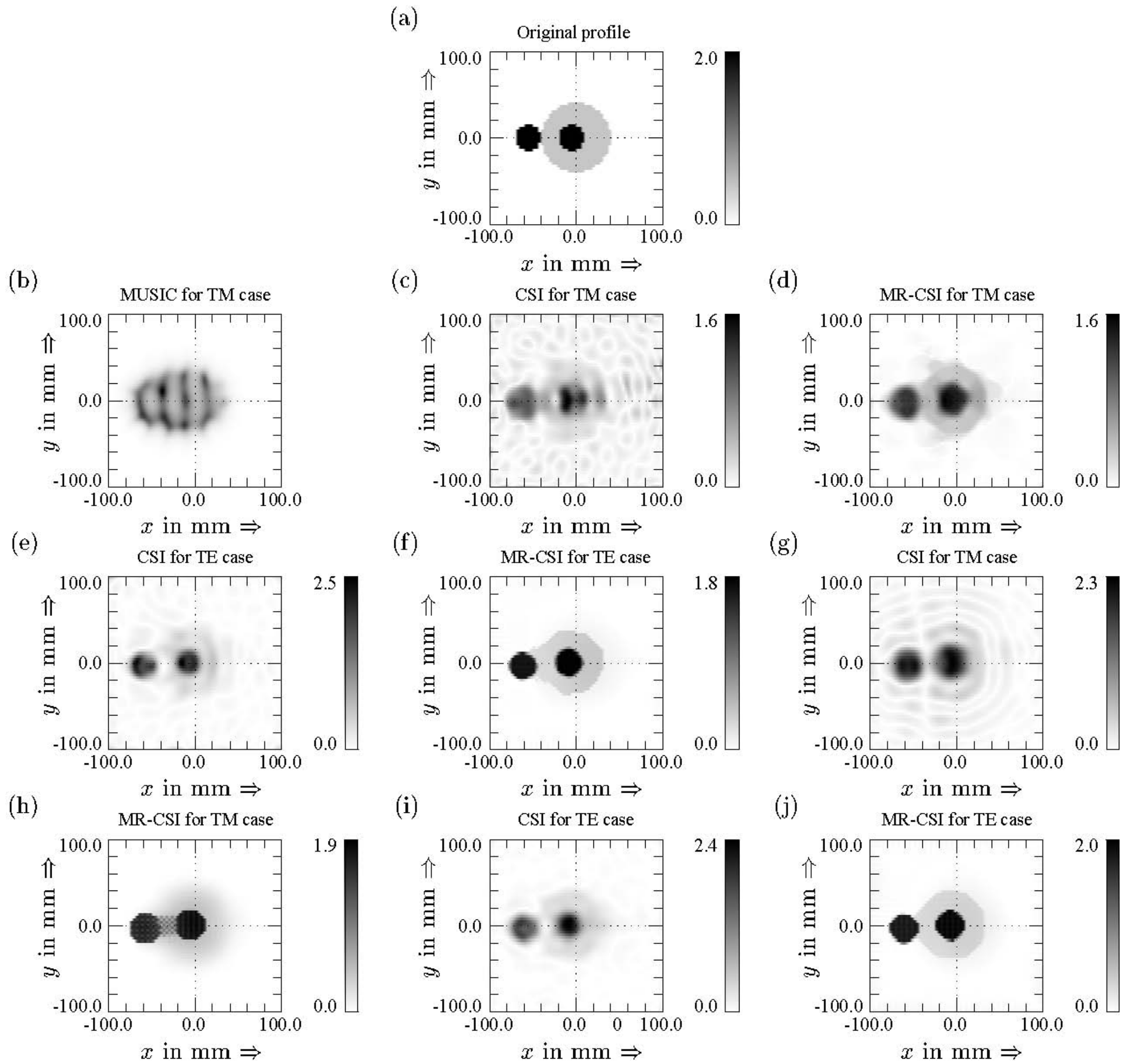

Fig. 1. MUSIC, CSI, and MR-CSI inversion results for experimental electromagnetic data. (a): Original profile. (b), (c), (d), (e) and (f): results obtained for a single frequency at $f = 6$ GHz. (g), (h), (i), and (j): results archived by applying the concurrent frequency (CF) approach with the data at $f = 2, 3, 4, 5, 6$ GHz. Except the MUSIC, the other results are obtained after 512 iterations.

5. A. Devaney, "Super-resolution processing of multi-static data using time reversal and MUSIC", Northeastern University, 2000.
6. M. Cheney, "The Linear Sampling Method and the MUSIC Algorithm", *Inverse Problems*, Vol. 17, pp. 591–595, 2001.
7. A. Kirsch, "The Extension of the MUSIC Algorithm to the Inverse Scattering Problem for Inhomogeneous Media", *Inverse Problems*, Vol. 16, pp. 89-105, 2000.
8. R. E. Kleinman and P. M. van den Berg, "A contrast source inversion method", *Inverse Problems*, Vol. 13, pp. 1607-1620, 1997.
9. R. Marklein, K. Balasubramanian, A. Qing and K. J. Langenberg, "Linear and nonlinear iterative scalar inversion of multi-frequency multi-bistatic experimental electromagnetic scattering data", *Inverse Problems*, Vol. 17, No. 6, pp. 1597-1610, 2001.

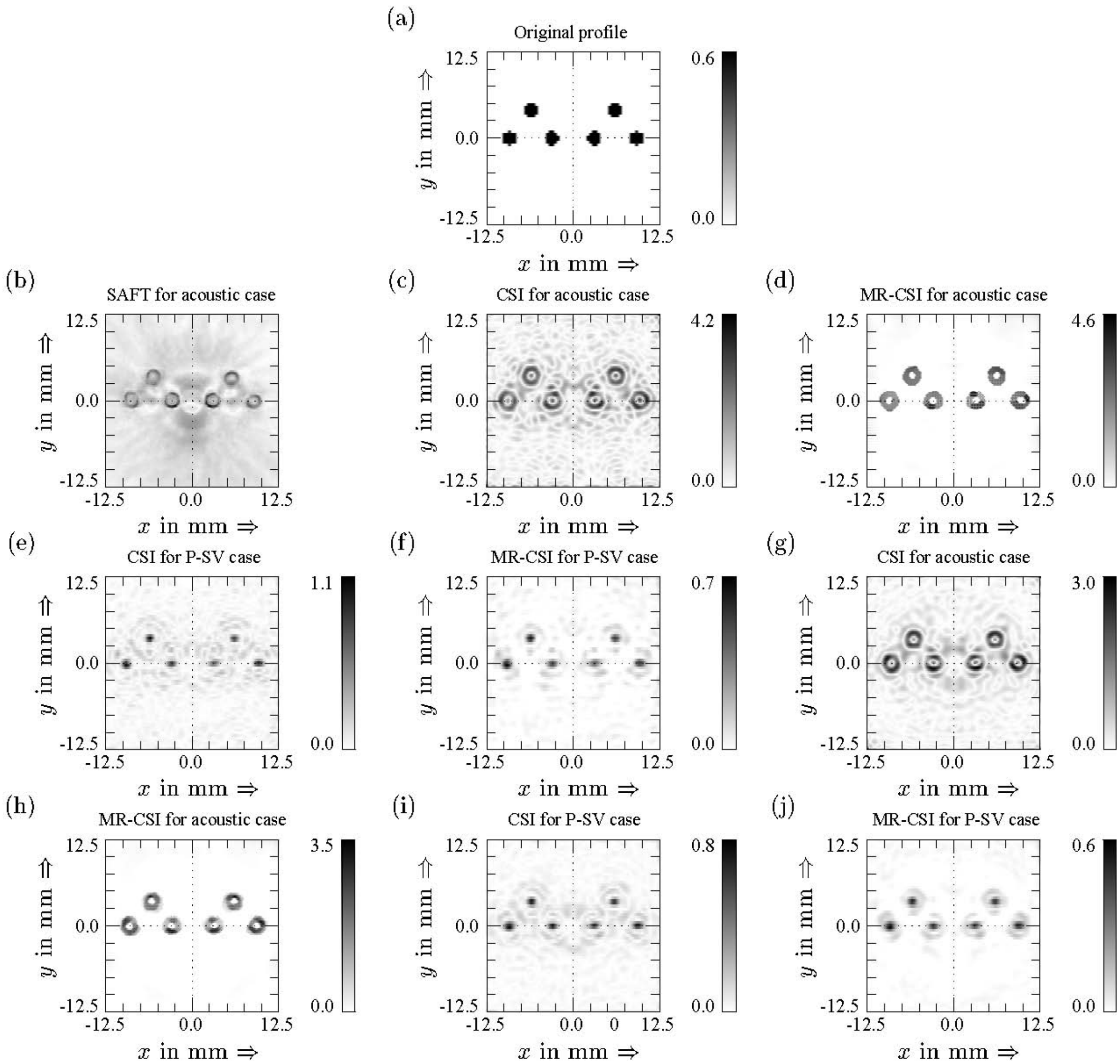

Fig. 2. SAFT, CSI, and MR-CSI inversion results for experimental elastic data. (a): Original profile. (c), (d), (e), and (f): results obtained at a single frequency of $f = 2.1$ MHz. (g), (h), (i), and (j): results obtained using the data at the frequencies $f = 1.9, 2.1, 2.3, 2.5, 2.7$ MHz are all added up, averaged and plotted. Except the SAFT, the other results are obtained after 256 iterations.

10. A. Abubarkar and P. M. van den Berg, "Iterative forward and inverse algorithms based on domain integral equations for three dimensional electric and magnetic objects", *Journal of Computational Physics*, Vol. 195, pp. 236-262, 2004.
11. G. Pelekanos, A. Abubakar and P. M. van den Berg, "Contrast source inversion methods in elastodynamics", *Journal of the Acoustical Society of America*, Vol. 114, pp. 2825-2834, 2003.
12. P. M. van den Berg and R. E. Kleinman, "A total variation enhanced modified gradient algorithm for profile reconstruction", *Inverse Problems*, Vol. 11, pp. L5-10, 1995.
13. A. Abubarkar, P. M. van den Berg and J. J. Mallorqui, "Imaging of biomedical data using a multiplicative regularized contrast source inversion method", *IEEE Transactions on Microwave Theory and Techniques*, Vol. 50, pp. 1761-1771, 2002.